Research Article

For reprint orders, please contact: reprints@futuremedicine.com

Nanomedicine

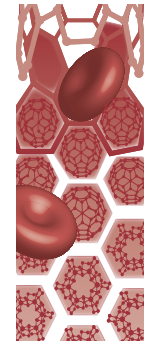

Oral administration of ginger-derived nanolipids loaded with siRNA as a novel approach for efficient siRNA drug delivery to treat ulcerative colitis

Aim: To develop novel siRNA delivery system overcoming the limitations of synthetic nanoparticles, such as potential side effects, nonspecificity and economic production for ulcerative colitis therapy. **Materials & methods:** Nanoparticles composed of edible ginger-derived lipid, termed ginger-derived lipid vehicles (GDLVs) were generated from ginger lipids through hydration of a lipid film, a commonly used method for a liposome fabrication. The morphology, biocompatibility and transfection efficiency of GDLVs loaded with siRNA-CD98 (siRNA-CD98/GDLVs) were characterized by standard methods. **Results:** Orally administered siRNA-CD98/GDLVs were effectively targeted specifically to colon tissues, resulting in reduced expression of CD98. **Conclusion:** These GDLVs have great promise as efficient siRNA-delivery vehicles while potentially obviating issues related to the traditional synthetic nanoparticles. As such, they help shift the current paradigm of siRNA delivery away from artificially synthesized nanoparticles toward the use of naturally derived nanovehicles from edible plants.

Mingzhen Zhang*[,1], Xiaoyu Wang[3], Moon Kwon Han[1], James F Collins[3] & Didier Merlin[1,2]

[1]Institute for Biomedical Sciences, Center for Diagnostics & Therapeutics, Georgia State University, Atlanta, GA 30302, USA
[2]Alanta Veterans Affairs Medical Center, Decatur, GA 30033, USA
[3]Food Science & Human Nutrition Department, University of Florida, Gainesville, FL 32611, USA
*Author for correspondence:
Tel.: +1 404 413 3597
Fax: +1 404 413 3580
mzhang21@gsu.edu

First draft submitted: 26 May 2017; Accepted for publication: 21 June 2017; Published online: 30 June 2017

Keywords: ginger-derived lipids vehicles • natural delivery system • oral administration • siRNA

Ulcerative colitis (UC) is a chronic inflammatory bowel disease (IBD) distinguished by inflammation of the large intestine (rectum and colon), typified by acute pain, vomiting, weight loss, diarrhea and bloody stool [1]. UC is associated with recurrent attacks that may last several months to years [2], giving rise to long-term complications that include decreased quality of life and productivity and an increased risk of colorectal cancer [3,4]. UC is typically treated with agents such as 5-aminosalicylic acid, sulfasalazine (SASP), steroid hormones, TNF-α inhibitors and immunosuppressive agents. Most of these therapies have side effects or are costly [5,6]. Despite the efficacy of these medications, their use has been limited by their nonspecific effects on the immune system, which result in short- and long-term pathophysiologic outcomes [7–9]. Further, anti-inflammatory drugs that are locally active with minimal systemic absorption (e.g., 5-aminosalicylic acid) require frequent intake of high doses to have measurable clinical activity. Accordingly, UC is classified by WHO as a refractory disease [10,11].

Molecular targeted therapeutic approaches based on the pathophysiology of inflammatory responses in IBD have been developed in the past decade. For example, inhibitors which target the pro-inflammatory cytokine TNF-α and suppress T-lymphocyte trafficking into the gut epithelium have been developed [12,13]. Indeed, anti-TNF-α agents are among the most potent drugs for the treatment of IBD. However, these drugs need to be administered systemically, and their use is limited by deleterious side effects [14]. There is thus an unmet need for a targeted carrier system capable of delivering low doses of drug specifically and effectively to the inflamed

Future Medicine part of fsg

regions for prolonged time periods. Such a delivery system could significantly reduce the off-target effects of existing, but otherwise effective, treatments.

Our laboratory and other groups have recently demonstrated that artificially synthesized nanoparticles may be used to target low doses of biological therapeutics, such as small interfering RNAs (siRNAs), proteins and peptides, to specific colonic cell types (e.g., epithelial cells and macrophages) [15–22]. However, the nanoparticles synthesized to date have two major limitations: each constituent of the synthetic nanoparticles must be examined for potential *in vivo* toxicity before clinical application; and production-scale synthesis of nanoparticles is problematic. We and others have developed natural nanoparticles that may overcome these two major limitations of synthetic nanoparticles. For example, we recently showed that a specific subpopulation of ginger nanoparticles is capable of reducing colitis and colitis-associated cancer [23,24]. However, the active compounds in ginger nanoparticles that provide these anti-inflammatory effects are not well defined.

In the present study, we established and characterized natural nanoparticles with a specifically defined drug cargo. To this end, we extracted lipids from ginger nanoparticles and loaded them with siRNA against CD98 (siRNA-CD98). We then investigated the ability of these siRNA-loaded 'natural liposomes' to target the colon. We chose to target CD98 because it is expressed in both the small and large intestine, and its increased colonic expression plays an important role in colitis and colitis-associated cancer, as shown by us and others [25–29]. Importantly, decreased expression of CD98 reduces colitis and colitis-associated cancer [25]. Our findings indicate that the natural nanoparticle carrier for a specific delivery of siRNA-CD98 to the colon, described here, could be a versatile therapeutic approach for treating UC.

Materials & methods

Materials

Edible ginger (*Zingiber officinale*) was purchased from a local farmer's market (GA, USA). Commercially available DC-Chol/DOPE blend was purchased from Avanti Polar lipids (AL, USA). Ascorbic acid, phalloidin-fluorescein isothiocyanate (FITC) and phosphorus standard solution were purchased from Sigma (MO, USA). Annexin V-FITC/ propidium iodide (PI) apoptosis detection kit was obtained from Molecular Probes (Eugene, OR, USA). Lipofectamine 2000, TurboFect *in vivo* Transfection Reagent and Quant-iT™ RiboGreen® RNA Assay Kit were purchased from Thermo Fisher Scientific (MA, USA). The near-infrared fluorescent, lipophilic carbocyanine (DiR) was purchased from PromoKine (Heidelberg, Germany). Negative control (scrambled) and positive CD98 siRNA were purchased from Santa Cruz (CA, USA).

Isolation & purification of ginger-derived nanoparticles

Ginger-derived nanoparticle (GDNP) isolation and purification were performed according to established methods [23]. Briefly, ginger was homogenized in a blender to obtain juice. The juice was then centrifuged at 3000 × *g* for 20 min and then 10,000 × *g* for 40 min with a Type 45Ti rotor to remove large fiber. The resulting supernatant was further spun at 150,000 × *g* for 2 h, and the pellet was then suspended in phosphate-buffered saline (PBS) and sonicated. This suspension was transferred to a sucrose gradient (8, 30 and 45% [g/v]) and spun at 150,000 × *g* for another 2 h. The band between the 30 and 45% layers was harvested and denoted as GDNPs [30].

Lipidomic analysis of GDNPs

Lipid extract from GDNPs was submitted to the Lipidomics Research Center, Kansas State University (KS, USA) for analysis. Briefly, the lipid composition was determined using a triple quadrupole mass spectrometer (Applied Biosystems Q-TRAP; Applied Biosystems, CA, USA) as described in an online protocol [31].

Data for each molecular lipid species were presented in Figure 1 as molar % of the total lipids analyzed.

Phosphorus quantification

Phosphate in ginger-derived nanovectors (GDNVs) was quantified by using a standard phosphorus solution (0.65 mM, Sigma). First, different amounts of phosphate standard solutions (0, 6.5, 13, 26, 52 and 104 nmol) and GDNV samples were added in glass test tubes, then 30 µl 10% $Mg(NO_3)_2.6H_2O$ (prepared in 95% alcohol) was added, and the mixture was heated by shaking the tubes over the strong flame of burden burner until the brown fumes disappeared. After cooling, 300 µl HCl (prepared in 0.5 N) was added to each tube and allowed to heat in a boiling water bath for 15 min to hydrolyze any pyrophosphate to phosphate. After the tube had cooled, 0.1 ml 10% ascorbic acid (prepared in ddH_2O) and 0.6 ml 0.42% ammonium molybdate.$4H_2O$ (prepared in 1 N H_2SO4) were added in sequence. Finally, the mix solutions were incubated at 45°C for 20 min and the absorbance was read at OD_{820}.

Ginger nanoparicle-derived lipid vectors/siRNA complexes preparation

First, total lipids were extracted using the Bligh and Dyer method [32]. Briefly, 6 ml of methyl alcohol/

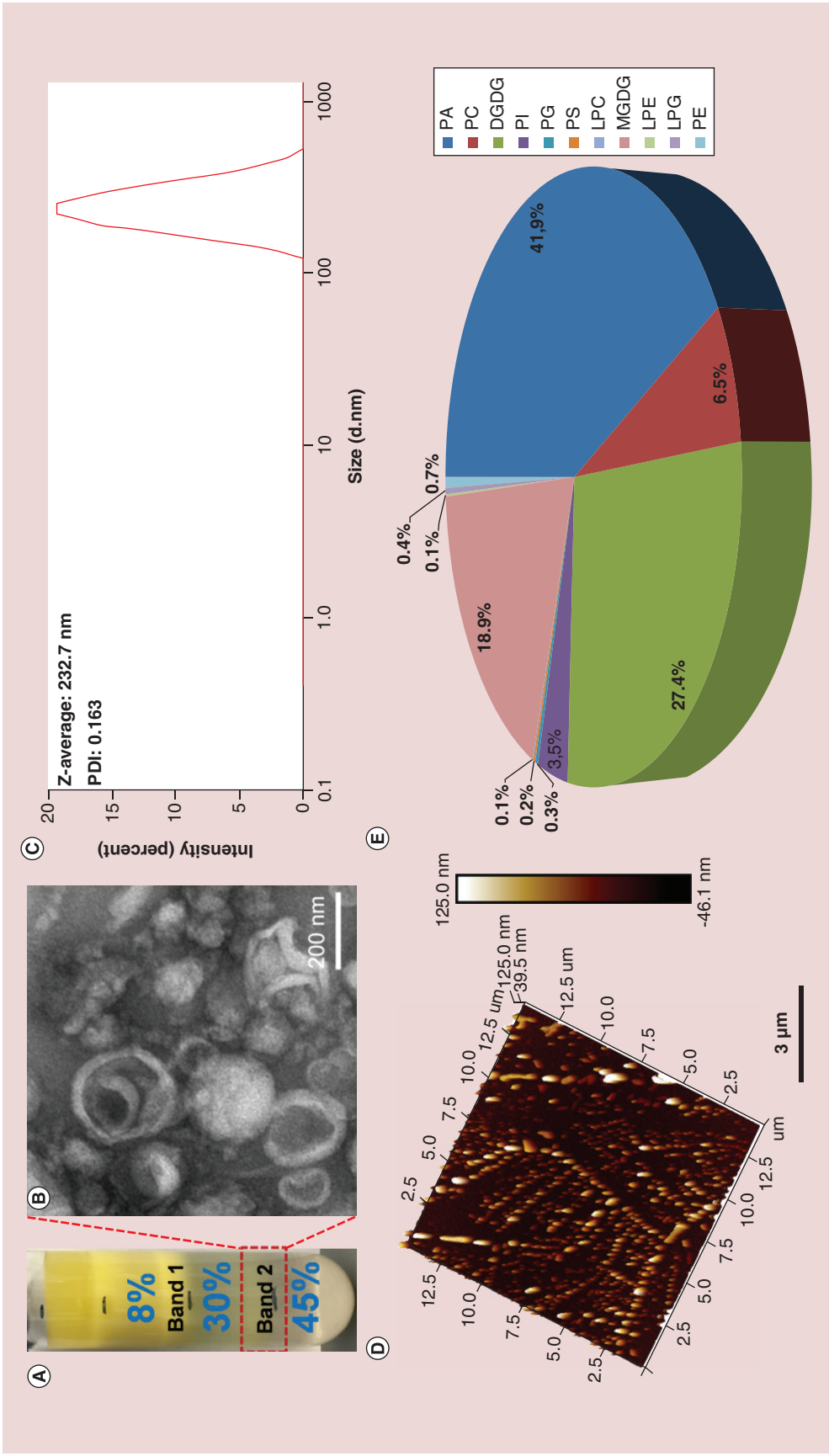

Figure 1. Identification and characterization of ginger-derived nanoparticles. Ginger rhizome/root-derived juice was purified by sucrose density gradient (8/30/45%) ultracentrifugation. **(A–D)** Band 2 from the 30/45% interface (red rectangle) was harvested and termed GDNPs **(A)**. GDNPs were characterized by TEM **(B)**, DLS **(C)** and AFM **(D)**. **(E)** Pie chart of the lipid profile of GDNPs as a percentage of total lipids (n = 5).
AFM: Atomic force microscopy; DGDG: Digalactosyldiacylglycerol; DLS: Dynamic light scattering; GDNP: Ginger-derived nanoparticle; LPC: Lysophosphatidylcholine; LPE: Lysophosphatidylethanolamine; LPG: Lysophosphatidylglycerol; MGDG: Monogalactosyldiacylglycerol; PA: Phosphatidic acid; PC: Phosphatidylcholine; PE: Phosphatidylethanolamine; PG: Phosphatidylglycerol; PI: Phosphatidylinositol; PS: Phosphatidylserine; TEM: Transmission electron microscopy.

chloroform at a volume ratio of 2:1 (v/v) was added to 1.6 ml of GDNPs (1 mg/ml) in PBS and shaken. Chloroform (2 ml) and ddH_2O (2 ml) were added sequentially. The mixture was centrifuged at 2000 rpm for 10 min at room temperature in glass tubes to separate the mixture into two phases (aqueous and organic). For collection of the organic phase, a glass pipette was inserted through the aqueous phase with gentle positive pressure and the bottom phase (organic phase) was aspirated and dispensed into fresh glass tubes. Then the samples were washed once with 0.5 ml of 1M KCl and once with 0.5 ml of ddH_2O. Finally, the organic phase samples were dried using rotary evaporators. For ginger nanoparticle-derived lipid vectors (GDLVs)/siRNA preparation, residual chloroform was removed using a vacuum pump for 2 h and the dried lipids were immediately suspended in 500 µl of 20 mM HEPES buffer, pH 7.4, and siRNAs were added. After sonicating for 5 min, an equal volume of HEPES buffer was added and the mixture was sonicated for another 5 min. Finally, the solution was passed through an AVES-TIN liposomes extruder with 200 nm polycarbonate membrane for 20-times (Ottawa, ON, Canada).

Transmission electron microscopy, atomic force microscopy & size measurements

For transmission electron microscopy (TEM) imaging, a drop of samples was deposited onto the surface of formvar-coated copper grids, and then 1% uranyl acetate was added for 15 s, the samples were allowed to dry at room temperature. Atomic force microscopy (AFM) images were obtained using a SPA 400 AFM (Seiko Instruments, Inc, Chiba, Japan). Particles size was measured using a Malvern Zetasizer Nano ZS90 Apparatus (Malvern Instruments, Worcestershire, UK) at room temperature.

siRNA loading efficiency

The loading efficiency of siRNA was determined using Quant-iT RiboGreen Reagent kit. Briefly, GDLVs–siRNA complex was diluted in TE buffer to a final volume of 1 ml. Then, 1 ml of aqueous working solu-

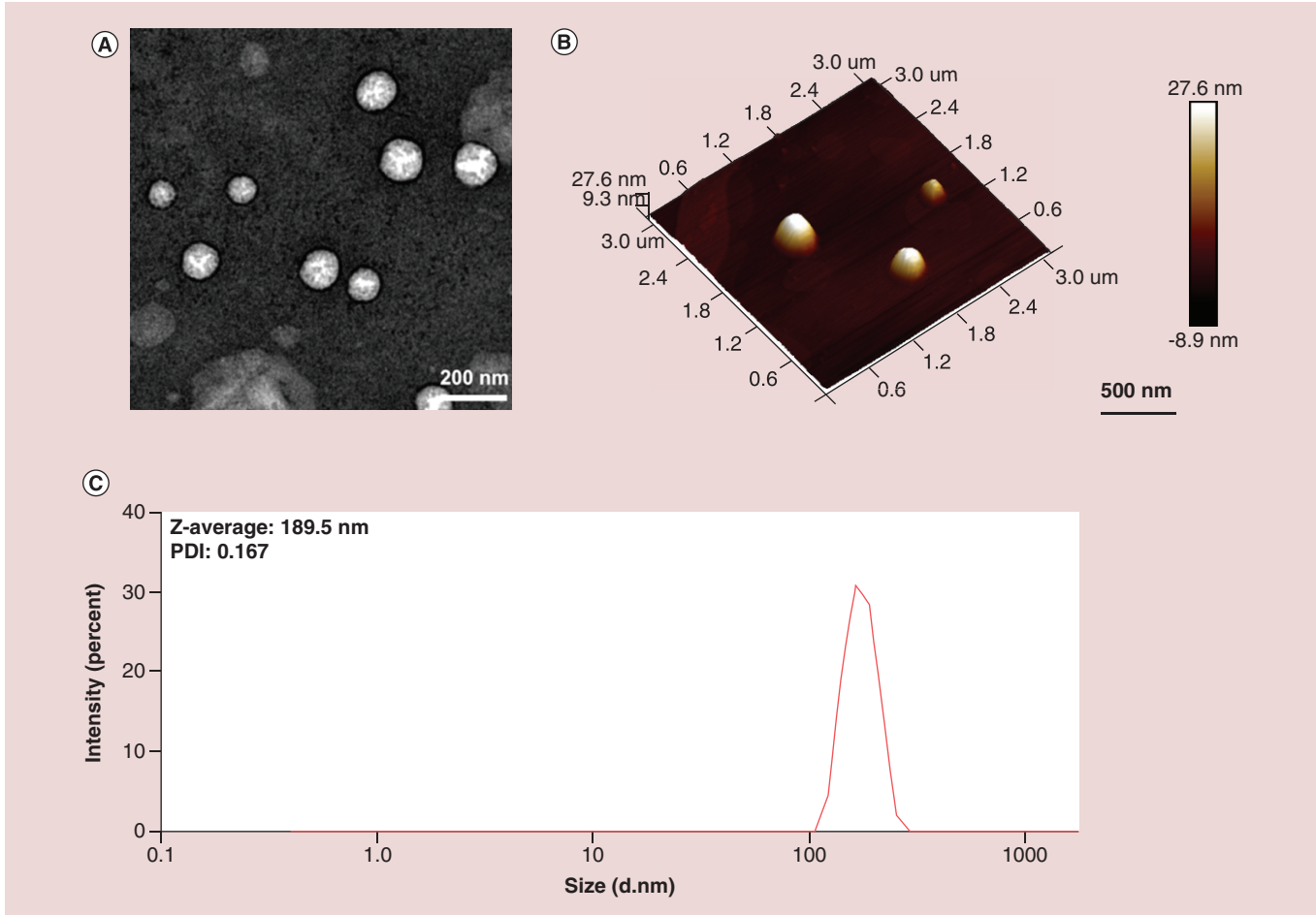

Figure 2. Characterization of ginger-derived lipid vehicles by transmission electron microscopy (A), atomic force microscopy (B) and dynamic light scattering (C).

tion of Quant-iT RiboGreen Reagent was added and the mixture was incubated for 5 min at room temperature in the dark. Finally, fluorescence of the samples was measured using fluorescence microplate reader (BioTek, Synergy2, USA) using standard fluorescein wavelengths (excitation ~480 nm; emission ~520 nm).

Cell culture

Caco-2BBE, RAW 264.7 and colon-26 cells were grown to confluence in 75 cm^2 flasks at 37°C in a humidified atmosphere containing 5% CO_2. Caco-2BBE and RAW 264.7 cells were cultured in DMEM and colon-26 cells were culture in RPMI 1640 medium (Life Technologies, NY, USA), media were supplemented with penicillin (100 U/ml), streptomycin (100 U/ml) and heat-inactivated fetal bovine serum (10%) (Atlanta Biologicals, GA, USA).

Cell proliferation assay

For *in vitro* toxicity analysis of GDLVs and DC-Chol/DOPE liposomes, MTT cell proliferation assay was used to assess the viability of RAW 264.7 and colon-26 cells. Briefly, cells were seeded in 96-well plates at a density of 1 × 10^4 cells/well and incubated overnight in standard medium. Different amounts of GDNVs or liposomes (5, 10, 20, 50, 100 and 200 µM) were added to each well and plates were incubated for 24 h. Then, 20 µl of MTT solution (5 mg/ml in PBS) was added to each well and the plates were incubated for another 4 h. Finally, the plates were shaken thoroughly for 1 min on the shaker, and measured the absorbance at 480 nm using a microplate reader.

Electrical impedance sensing assay

Cell attachment assays were performed to investigate real-time cytotoxicity using electrical impedance sensing (ECIS) technology (Applied BioPhysics, NY, USA), which is based on AC impedance measurements. The attachment and spread of cells on the electrode surface changes the impedance in such a way that morphological information about attached cells can be inferred. The measurement system consists of an eight-well cul-

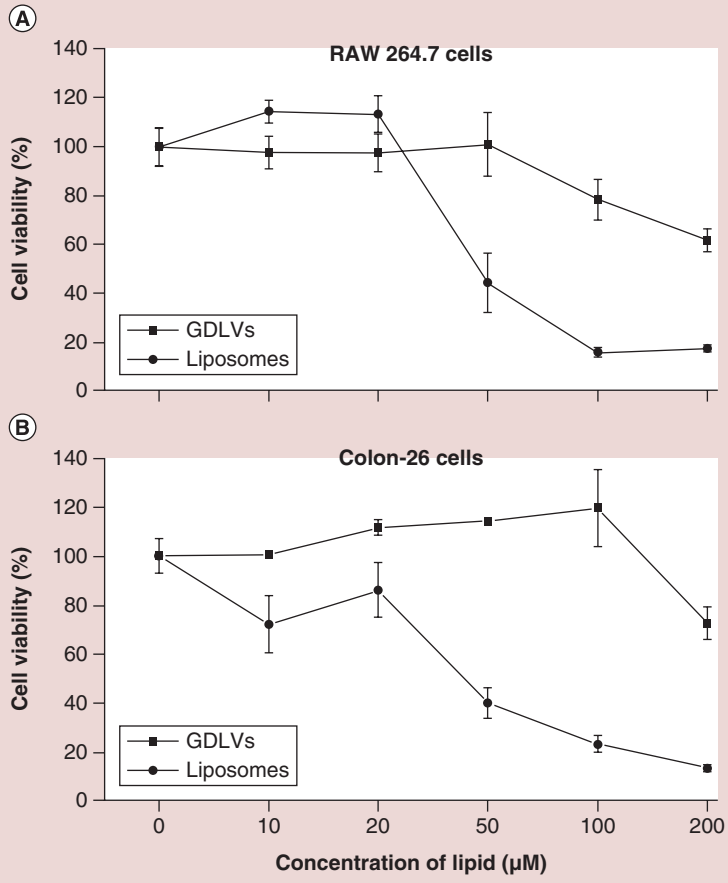

Figure 3. Ginger-derived lipid vehicles are biocompatible. The viability of RAW 264.7 cells **(A)** and colon-26 cells **(B)** was evaluated after incubating with GDLVs or DC-Chol/DOPE liposomes for 24 h.
GDLV: Ginger-derived lipid vehicle.

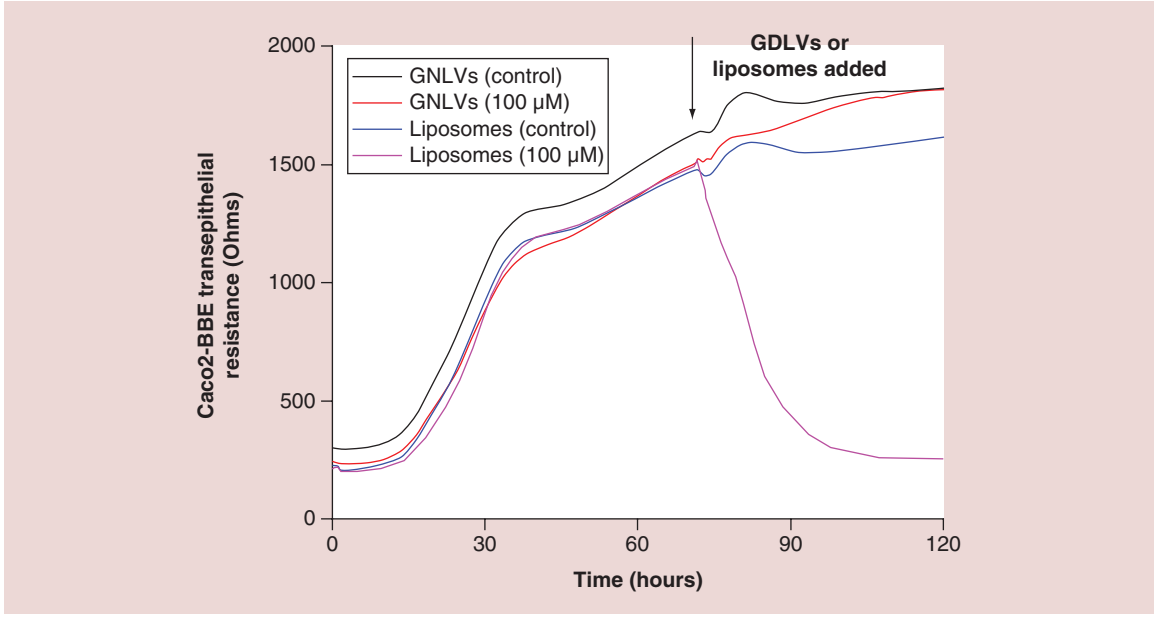

Figure 4. Ginger-derived lipid vehicles do not affect the integrity of intestinal barrier function. GDLVs (100 μM), DC-Chol/DOPE liposomes (100 μM) or control (PBS) were added, as indicated by arrows.
GDLV: Ginger-derived lipid vehicle; PBS: Phosphate-buffered saline.

ture dish (ECIS 8W1E plate) with the surface treated was used for cell culture. For experiment, Caco2-BBE cells were seeded at a density of 2 × 10^5/well on the plate. Once cells reached confluence, PBS (control), GDLVs (100 μM) or liposome (100 μM) was added to the wells. Basal resistance measurements were performed using the ideal frequency for Caco2-BBE cells, 500Hz and a voltage of 1V.

Cell apoptosis study

Apoptosis of cells *in vitro* was determined by an Annexin V-FITC/PI double staining assay. For fluorescence imaging, colon-26 and RAW 264.7 cells were seeded on eight-chamber slides (Tissue-Tek; Sakura, USA) and cultured overnight at 37°C. Then, cells were treated with GDLVs (100 μM) or liposome (100 μM) for 8 h. After treatment, cells were collected and washed with chilled PBS. Annexin V binding buffer (500 μl) was mixed with 5 μl of Annexin V-FITC and PI, and was added to the cells, followed by incubation at room temperature in the dark for 15 min. Then, stained cells were counterstained by 4-, 6-diamidino-2-phenylindole (DAPI) to allow visualization of nuclei. Samples were then visualized using fluorescence microscopy.

For flow cytometry, colon-26 and RAW 264.7 cells were stained with Annexin V-FITC and PI following the same protocol as in fluorescence imaging and analyzed with a FACS Canto flow cytometer (BD Biosciences, CA, USA). Healthy cells were double negative for Annexin V and PI staining, and early apoptotic cells were positive for Annexin V but negative for PI staining and necrotic cells were positive only for the PI while late apoptotic cells were doubly positive. The excitation wave length was set at 488 nm and the emission of green fluorescence of Annexin V and red fluorescence of PI were collected using 525 and 575 nm band pass filters, respectively. Triplicate samples were analyzed in each experiment.

Blood hemanalysis & biochemical analysis

Blood samples were collected from different (PBS and GDLVs) treated groups. Blood cells and biochemical analyses were performed using a hematology analyzer (VetScan HM5; Abaxis, CA, USA) and a biochemical analyzer (VetScan VS2; Abaxis), respectively.

Cell uptake of GDLVs/siRNA-FITC

For confocal imaging of cellular uptake of GDLVs/

Figure 5. Ginger-derived lipid vehicles do not induce apoptosis in RAW 264.7 cells (see facing page).
(A) Fluorescence images of RAW 264.7 cells treated with GDLVs (100 μM) or liposomes (100 μM) for 8 h.
(B & C) Flow cytometry analysis of apoptotic cells **(B)** and quantification of the PI^-/$Annexin^-$ double-negative cell population from B **(C)**.
GDLV: Ginger-derived lipid vehicle.
Data are from three independent experiments.

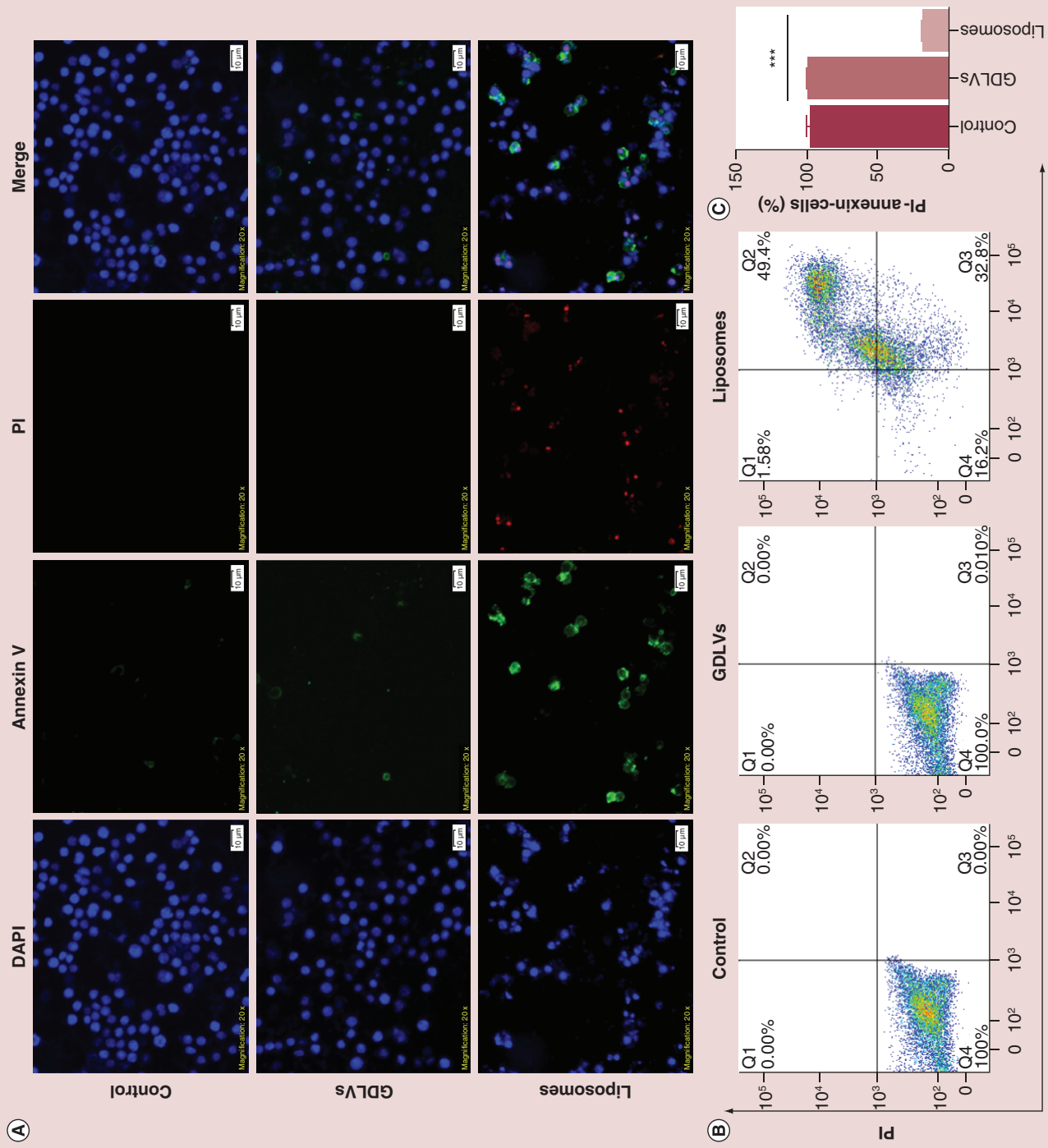
A
DAPI
Annexin V
PI
Merge
Control
GDLVs
Liposomes
Magnification: 20 x
10 μm
B
Control
GDLVs
Liposomes
PI
Annexin V
Q1 0.00%
Q2 0.00%
Q3 0.00%
Q4 100%
Q1 0.00%
Q2 0.00%
Q3 0.010%
Q4 100.0%
Q1 1.58%
Q2 49.4%
Q3 32.8%
Q4 16.2%
C
PI-annexin-cells (%)
***
Control
GDLVs
Liposomes

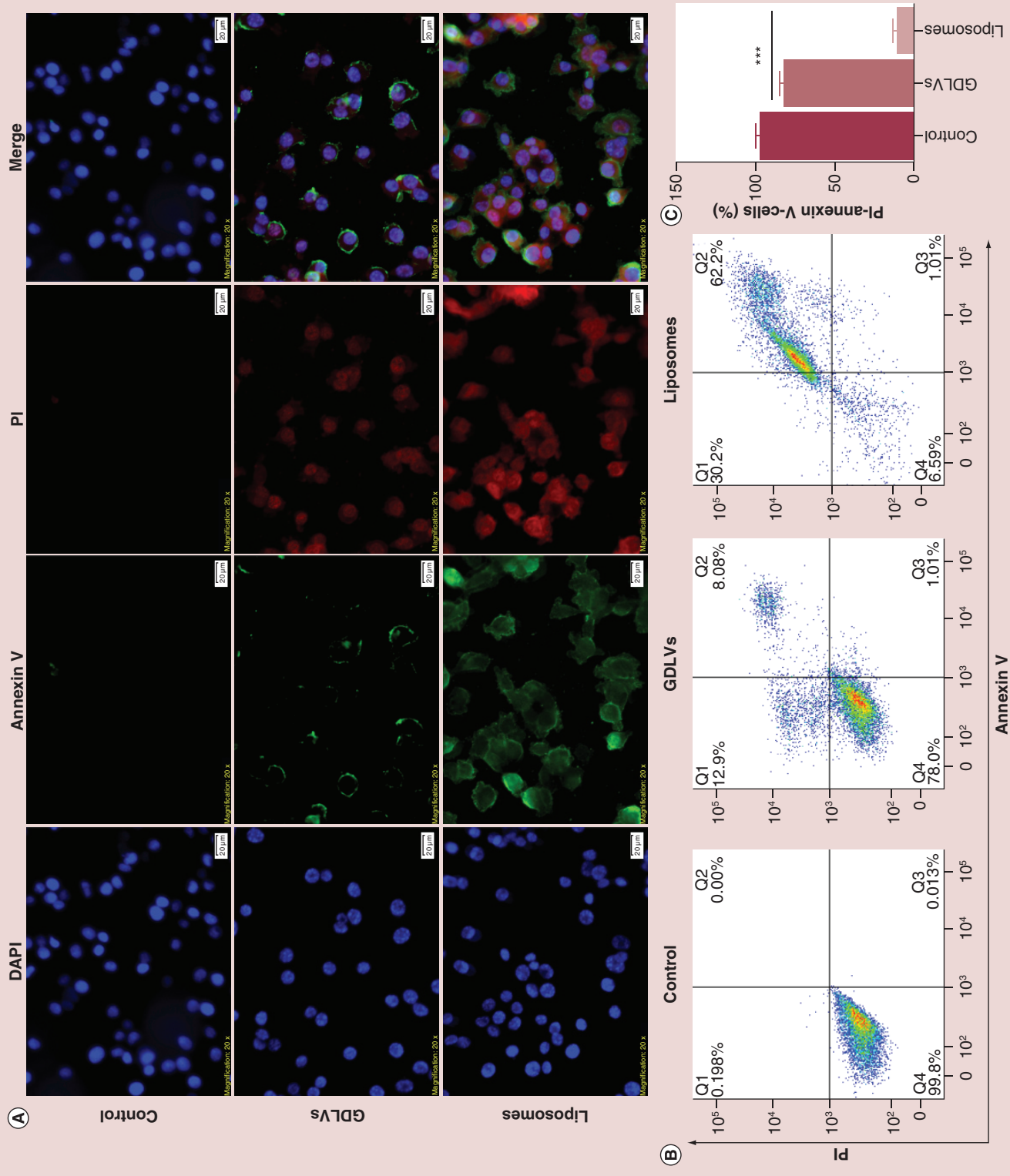
A
DAPI
Annexin V
PI
Merge
Control
GDLVs
Liposomes
B
Control
GDLVs
Liposomes
PI
Annexin V
Q1 0.198%
Q2 0.00%
Q3 0.013%
Q4 99.8%
Q1 12.9%
Q2 8.08%
Q3 1.01%
Q4 78.0%
Q1 30.2%
Q2 62.2%
Q3 1.01%
Q4 6.59%
C
PI-annexin V-cells (%)
***
Control
GDLVs
Liposomes

Figure 6. Ginger-derived lipid vehicles do not induce apoptosis in colon-26 cells. (A) Fluorescence images of colon-26 cells treated with GDLVs (100 μM) or liposomes (100 μM) for 8 h. **(B & C)** Flow cytometry analysis of apoptotic cells **(B)** and quantification of the $PI^-/Annexin^-$ double-negative cell population from B **(C)**.
GDLV: Ginger-derived lipid vehicle.
Data are from three independent experiments.

siRNA-FITC, Colon-26 and RAW 264.7 cells were seeded at 1 × 10^5/well on eight-chamber slides (Tissue-Tek; Sakura) and cultured overnight at 37°C. Then, medium was removed, cells were rinsed with PBS, and Opti-MEM containing GDLVs/siRNA-FITC (15 pmol/well siRNA-FITC) was added. After 8-h incubation, the cells were washed and fixed with 4% paraformaldehyde for 15 min. and then dehydrated with acetone at -20°C for 5 min. After blocking with 1% bovine serum albumin in PBS for 30 min, 100 μl of phalloidin-FITC (1:40 dilution) was added and the cells were incubated for an additional 30 min. Finally, cells were coverslip-mounted with mounting medium containing DAPI. Cells were observed and imaged using a Zeiss LSM 700 confocal microscope with Zen 2014 software version 9.1.

In vitro gene silencing

Colon-26 cells and RAW 267.4 macrophage were seeded at 1 × 10^5/well in 12-well plates and incubated overnight. Cells were then co-cultured with CD98 siRNA, lipofectamine 2000 plus CD98 siRNA (Lipo 2000/CD98 siRNA), GDLVs or GDLVs plus CD98 siRNA (GDLVs/CD98 siRNA) for 24 h and 48 h. the siRNA concentration was 30 nM. Cells were subsequently harvested and mRNA expression levels were qRT-PCR using Maxima SYBR green/6-carboxy-X-rhodamine (ROX) qPCR Master Mix (Thermo Scientific). The data were normalized to the internal control 36B4. Relative gene expression levels were calculated using the $2^{-\Delta\Delta Ct}$ method. The primer sequences were as follows:

- mCD98 forward:
  5′-GAGGACAGGCTTTTGATTGC-3′
- mCD98 reverse:
  5′-ATTCAGTACGCTCCCCAGTG-3′
- 36B4 forward:
  5′-TCCAGGCTTTGGGCATCA-3′
- 36B4 reverse:
  5′-CTTTATCAGCTGCACATCACTCAGA-3′

Biodistribution of GDLVs in mouse intestinal tract

For the biodistribution of GDLVs in mouse intestinal tract, mice were orally gavaged with DiR-labeled GDLVs and imaging of the intestinal tract was done at 12 h after the oral administration. The intensity of DiR signal from different samples was then measured using an IVIS series preclinical *in vivo* imaging systems (PerkinElmer, MA, USA).

In vivo transfection of GDLVs–siRNA complex

For *in vivo* transfection, siRNA (3.3 nmol) was dissolved in 300 μl sterile 5% glucose solution, vortexed gently and spun down. Then, TurboFect reagent was then added (6 μl) to the diluted siRNA, and it was mixed immediately and incubated for 15 min at room temperature. The packed siRNA/TurboFect was then added to the lipid film of ginger with sonication to pre-

Table 1. Safely evaluation of ginger-derived lipid vehicles *in vivo* was evaluated by analyzing hematology and biochemistry parameters (mean ± standard deviation, n = 3).

Analytes	Phosphate-buffered saline group	Ginger-derived lipid vehicles group
WBC (×10^9/l)	10.36 ± 3.4	8.30 ± 2.3
LYM (×10^9/l)	9.78 ± 1.2	7.70 ± 2.5
MON (×10^9/l)	0.22 ± 0.01	0.25 ± 0.04
NEU (×10^9/l)	0.36 ± 0.05	0.35 ± 0.15
RBC (×10^{12}/l)	9.76 ± 0.4	9.44 ± 0.5
HGB (×g/dl)	13.8 ± 1.0	13.7 ± 0.8
PLT (×10^9/l)	526 ± 45.8	504 ± 59.2
ALT (×U/l)	31 ± 1.9	34.5 ± 5.7
ALB (×g/dl)	4.2 ± 0.5	4.8 ± 0.6
ALP (×U/l)	153 ± 23	121 ± 31
AMY (×U/l)	754 ± 31	782 ± 21
CA (×mg/dl)	11.3 ± 0.7	12.0 ± 0.5
CRE (×mg/dl)	0.3 ± 0.05	0.2 ± 0.1
GLOB (×g/dl)	0.9 ± 0.1	1.0 ± 0.2
GLU (×mg/dl)	199 ± 25	174 ± 31
PHOS (×mg/dl)	9.0 ± 1.9	10.9 ± 0.8
K^+ (×mmol/l)	6.1 ± 0.7	6.8 ± 0.2
NA^+ (×mmol/l)	153 ± 1.5	152 ± 3.2
TBIL (×mg/dl)	0.3 ± 0.1	0.2 ± 0.2
TP (×g/dl)	5.1 ± 0.9	5.9 ± 0.5
BUN (×mg/dl)	30 ± 5	26 ± 4

Hematology parameters: ALT: Alanine aminotransferase; AST: Aspartate aminotransferase; HGB: Hemoglobin; LYM: Lymphocyte; MON: Monocyte; NEU: Neutrophil; PLT: Platelet; RBC: Red blood cell; WBC: Total white blood cell.
Biochemistry parameters: ALT: Alanine aminotransferase; ALB: Albumin; ALP: Alkaline phosphatase; AMY: Amylase; BUN: Blood urea nitrogen; CA: Calcium; CRE: Creatinine; GLOB: Globulin; GLU: Glucose; PHOS: Phosphorus; TBIL: Total bilirubin; TP: Total protein.

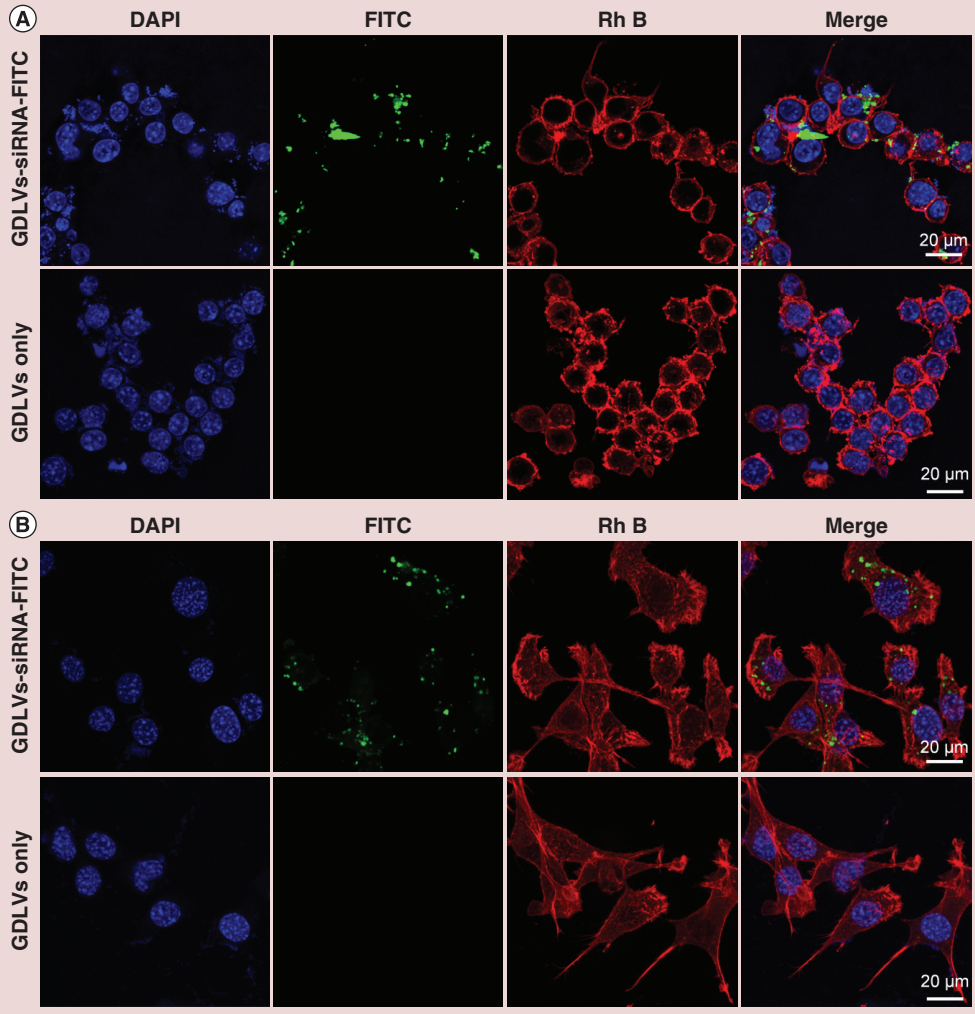

Figure 7. siRNA-fluorescein isothiocyanate/ginger-derived lipid vehicles are taken up by RAW 264.7 cells (A) and colon-26 cells (B).

pare GDLVs/siRNA. Finally, mice were orally administrated this solution twice (12 h apart). CD98 mRNA expression in different parts of intestinal tract (duodenum, jejunum, ileum and colon) was subsequently measured by standard qRT-PCR.

Statistical analysis

One- and two-way analyses of variance and *t*-tests were used to determine statistical significance (*$p < 0.05$; **$p < 0.01$; ***$p < 0.001$), as indicated in the figure legends.

Results & discussion

Characterization of GDNPs & GDLVs

GDNPs were first isolated and purified from homogenized ginger using ultracentrifugation and sucrose gradient centrifugation methods established in our laboratory [23]. The majority of the ginger extract accumulated at the 8/30% (band 1) and 30/45% (band 2) interfaces of the sucrose gradient. Nanoparticles from band 2 have been characterized previously and are referred to as GDNPs (Figure 1A) [33,34]. The integrity and size distribution of GDNPs were first evaluated by TEM (Figure 1B) and dynamic light scattering (DLS) analyses (Figure 1C). The results showed that GDNPs have an exosome-like structure with an average diameter of approximately 232.7 nm and a polydispersity index of 0.163. Further characterization of GDNPs by AFM (Figure 1D) yielded data that were consistent with those obtained using TEM and DLS. A lipidomic analysis (Figure 1E) indicated that GDNPs were enriched for phosphatidic acids (41.9% of total lipids), digalactosyldiacylglycerol (27.4%) and monogalactosyldiacylglycerol (18.9%). Recent research has shown that phosphatidic acids control membrane fission and fusion because of their small

negatively charged head group, which lies very close to the alkyl chain region of the bilayer, their high affinity for divalent cations and their propensity to form intermolecular hydrogen bonds [35,36]. Monogalactosyldiacylglycerol and digalactosyldiacylglycerol are important glycolipids, which can stabilize phospholipid liposomes during freeze-thawing/freeze-drying processes, making glycolipids an interesting potential stabilizer for liposome-encapsulated drugs or siRNA [37–40]. Varying amounts of other lipid components, such as phosphatidylcholine, phosphatidylinositol, phosphatidylglycerol, phosphatidylserine, lysophosphatidylcholine, lysophosphatidylethanolamine, lysophosphatidylglycerol and phosphatidylethanolamine were also found among GDNP-extracted lipids.

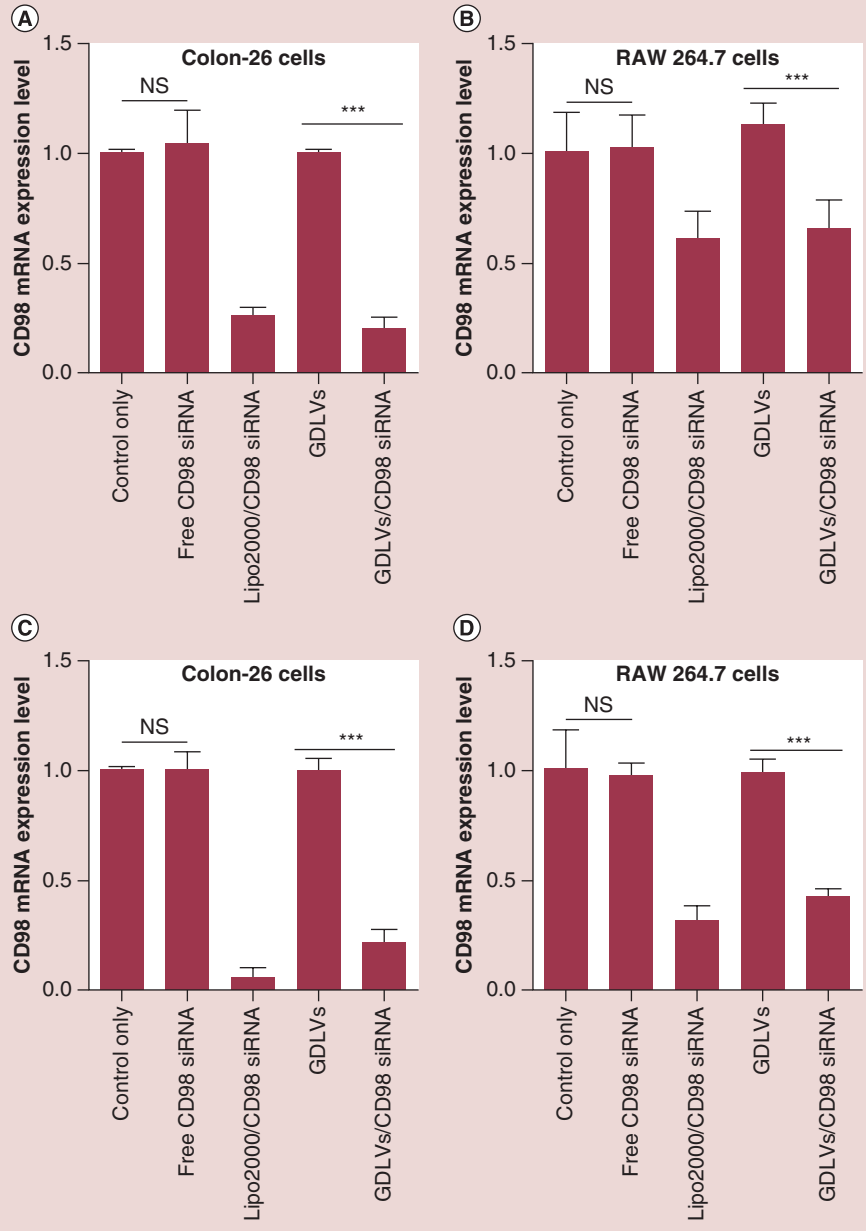

Figure 8. Ginger-derived lipid vehicles loaded with siRNA-CD98 reduce CD98 mRNA expression in colon-26 and RAW 264.7 cells. After incubating cells with free siRNA-CD98, Lipo2000/CD98 siRNA, GDLVs or siRNA-CD98/GDLVs for 24 and 48 h, CD98 mRNA expression levels were evaluated by real-time PCR. **(A)** Colon-26 cells at 24 h; **(B)** RAW 264.7 cells at 24 h; **(C)** Colon-26 cells at 48 h; **(D)** RAW 264.7 cells at 48 h (n = 5).
GDLV: Ginger-derived lipid vehicle.

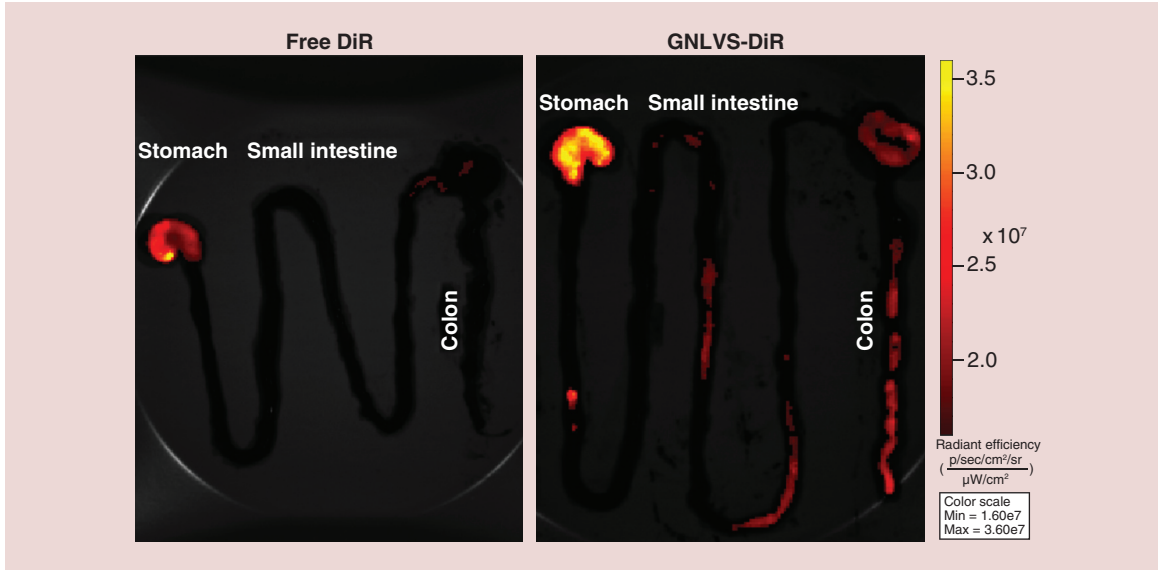

Figure 9. Orally administered DiR/ginger-derived lipid vehicles target the large intestine. Six-week-old female FVB mice were orally administered free DiR or DiR/GDLVs, and their digestive tracts were imaged 12 h after administration. Representative images are from three independent experiments (n = 3).
GDLV: Ginger-derived lipid vehicle.

To determine whether lipids from GDNPs could reassemble into nanosized particles and serve as therapeutic GDLVs, we employed a standard method based on hydration of a lipid film to fabricate liposomes. TEM and AFM images (Figure 2A & B) of GDLVs showed that these particles were nanosized and had a spherical shape. DLS analyses confirmed that GDLVs were nanosized with an average hydrodynamic diameter of approximately 189.5 nm and a relatively low polydispersity index of 0.167. ζ-potential data showed that GDLVs had a negative potential (-18.1 mV) and did not have significant change after loading siRNA (-18.4 mV) (Supplementary Figure 1). Moreover, we found that GDLVs were very stable and could be stored for up to 25 days at 4°C without any changes in size or ζ-potential – a property that is very important for lipid nanoparticles used for drug or siRNA delivery. Collectively, these results suggest that lipids derived from GDNPs can assemble into nanosized particles for potential drug- or siRNA-delivery applications.

GDLVs have good biocompatibility

Lipid nanoparticles are currently the favored vehicle for therapeutic siRNA delivery; however, synthetic lipid nanoparticles (e.g., liposomes) can lead to undesirable effects, such as cell stress, inflammasome activation and apoptosis [41]. Here, to assess the biocompatibility of GDLVs, we first used MTT assays to determine whether GDLVs were toxic to RAW 264.7 macrophage-like cells and colon-26 colonic cancer cells. The commercially available liposome preparation, DC-Chol/DOPE (30/70, w/w), which has been widely used for siRNA delivery [42–46], was used as a standard control. MTT results showed that, following a 24-h incubation, GDLVs had less of an effect on the viabilities of both cell lines than DC-Chol/DOPE (Figure 3), which dramatically reduced the viability of both RAW 264.7 and colon-26 cells in a lipid-concentration-dependent manner (up to 200 µM). As an alternative approach for evaluating the biocompatibility of GDLVs, we also employed ECIS technology to monitor the barrier function of Caco2-BBE human colorectal cancer cell monolayers. After Caco2-BBE cells had attached to the electrode surface to form a monolayer, GDLV or liposome nanoparticles were added at the same final concentration (100 µM) to individual wells in the plate; PBS was used as a control. As shown in Figure 4, GDLVs had less of an effect on intestinal barrier function than DC-Chol/DOPE liposomes, which showed a degree of toxicity toward intestinal epithelial cells at the same lipid concentration.

We also used an Annexin V/PI assay (Annexin V-FITC/PI) to quantify apoptosis as an additional method for evaluating the biocompatibility of GDLVs. Fluorescence microscopy revealed that GDLV-treated RAW 264.7 cells showed less positive staining for both Annexin V-FITC and PI (Figure 5A) than cells in the liposome-treated group; as expected no such signal was detected in untreated control cells. Quantification of flow cytometry results revealed that the $FITC^-/PI^-$ double-negative (healthy) cell population accounted for 97.7 ± 3.9%, 99.6.7 ± 0.57% and 18.6 ± 2.2% of

the total cell population in control, GDLV-treated and liposome-treated groups, respectively (Figure 5B & C). Four distinct phenotypes are distinguishable using this approach: viable cells (lower right quadrant); early

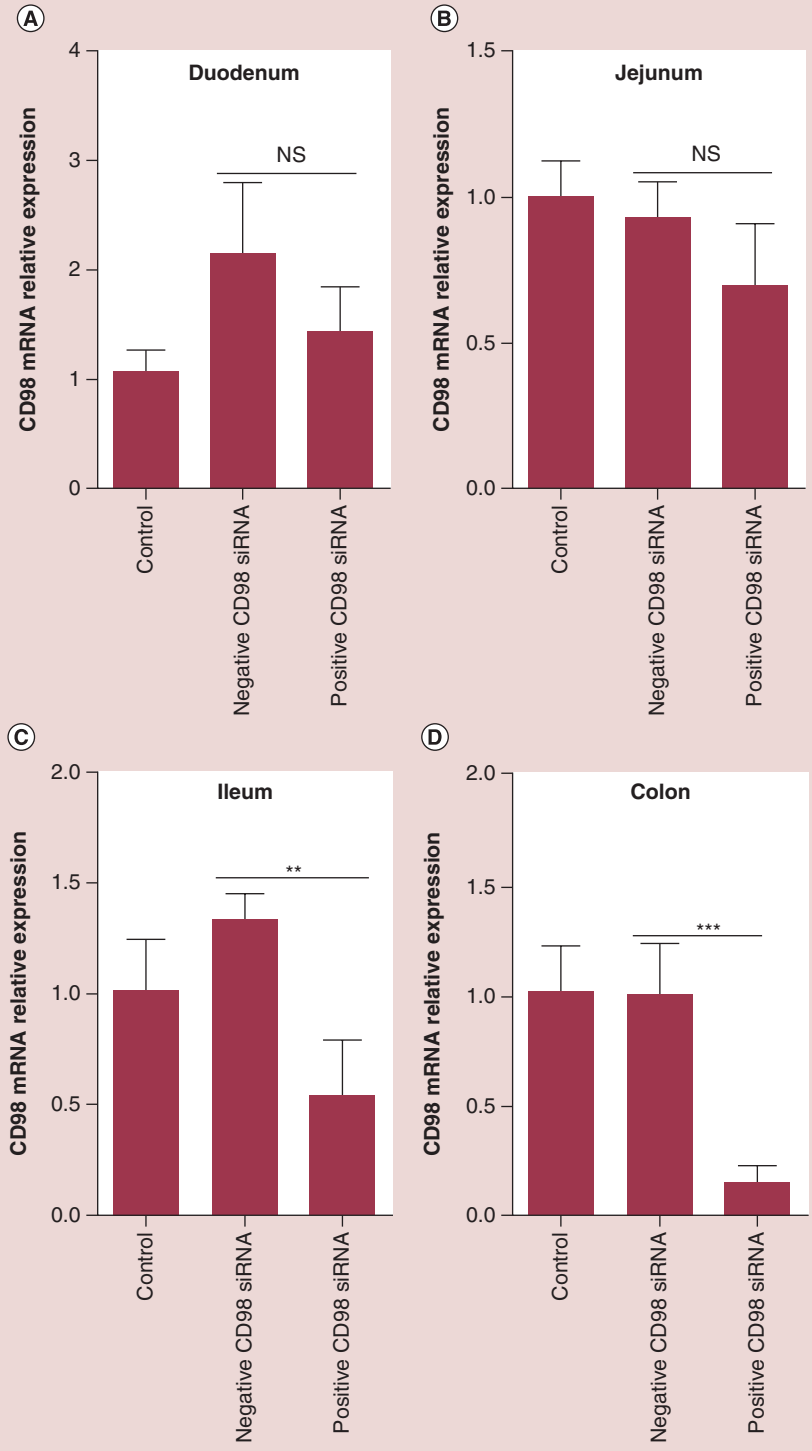

Figure 10. siRNA-CD98/GDLVs target the large intestine and effectively deliver siRNA-CD98 to colonocytes. After two oral administrations of siRNA-CD98/GDLVs (12 h apart), different parts of the digestive tract were collected and CD98 mRNA expression levels in the duodenum **(A)**, jejunum **(B)**, ileum **(C)** and colon **(D)** were evaluated using qRT-PCR (n = 5).
GDLV: Ginger-derived lipid vehicle.

apoptotic cells (lower right quadrant); necrotic cells (upper left quadrant); and apoptotic cells (upper right quadrant). Similar results were obtained in colon-26 cells, which exhibited $FITC^-/PI^-$ double-negative cell populations of 97.7 ± 3.8%, 82.3 ± 4.5% and 10.7 ± 4.4%, respectively (Figure 6). GDLVs with negative potential had better biocompatibility than cationic liposome-DC-Chol/DOPE. The possible reasons can be explained: cationic liposomes composed of cationic lipids, which are known to be membrane active. When incubating with cells, cationic lipids may interfere with the membrane function and integrity of the cell or the subcellular compartments and lead to toxicity. The presence of the pH-sensitive lipid DOPE in the liposome may be another reason to the toxicity. The success of transfection is determined by the intracellular fate following uptake into the cells; most of the complexes are degraded in the lysosomes. Due to the formation of an inverted hexagonal phase at acidic pH, a pH typically found in the lysosomes, DOPE may enhance the cationic lipid toxicity by destabilizing the lysosomal membrane. In addition, the cationic lipids can become cytotoxic by interacting with critical enzymes such as protein kinase C. Recent researches showed that many derivatives of cholesterol which contain tertiary or quaternary nitrogen headgroups can inhibit protein kinase C activity. Due to these possible reasons, GDLVs showed better biocompatibility than cationic liposomes.

Next, we evaluated the potential side effects of GDLVs *in vivo*. Blood from mice treated with PBS or GDLVs was collected for hemanalysis and biochemical analysis. As shown in Table 1, these analyses revealed no differences in the numbers of white blood cells, red blood cells, hemoglobin or hepatic and renal functional parameters, including blood urea nitrogen, total bilirubin, alanine aminotransferase and total protein, between PBS- and GDLV-treated groups, indicating that GDLVs are safe *in vivo*. Taken together, these results indicate that GDLVs are nontoxic compared with the commercial liposome preparation, DC-Chol/DOPE, and can be developed as a nontoxic siRNA-delivery vehicle.

GDLVs/siRNA-FITC are taken up by cells

Next, we investigated whether GDLVs could be taken up by RAW 264.7 and colon-26 cells. To this end, we used GDLVs loaded with FITC-tagged siRNA (siRNA-FITC/GDLVs) as a reporter to allow monitoring of cellular uptake by confocal microscopy; rhodamine B (RhB) phalloidin (red channel) and DAPI (blue channel) were used to stain the actin cytoskeleton and nucleus, respectively. As shown in Figure 7, after incubating with siRNA-FITC/GDLVs for 8 h, siRNA-associated fluorescence (green dots) was distributed throughout the cell in both RAW 264.7 and colon-26 cell groups. For example, the transfection effeciency for colon-26 cell group could be up to 62.8% (Supplementary Figure 2). As expected, there was no siRNA-associated fluorescence observed in the group receiving GDLV only, used as a negative control. Taken together, these observations indicate that siRNA-FITC/GDLVs can be taken up in a highly efficient manner by both RAW 264.7 and colon-26 cells, indicating that GDLVs can be employed as an siRNA-delivery vehicle without the use of toxic transfection reagents such as Lipofectamine.

GDLVs loaded with siRNA-CD98 effectively decrease CD98 expression

Although confocal images confirmed that siRNA-FITC was transported into the cytoplasm of RAW 264.7 and colon-26 cells after co-incubation with siRNA-FITC/GDLVs for 8 h, we wanted to determine whether siRNA-CD98 was encapsulated and delivered by GDLVs in a functional form. First, we calculated the entrapment efficiency of siRNA-CD98 into GDLVs using Quant-iT RiboGreen RNA reagent, one of the most sensitive fluorescent dyes for the quantification of RNA in solution. This analysis revealed an efficiency of siRNA-CD98 entrapment up to 61 ± 8%, indicating that GDLVs are an excellent siRNA-delivery vehicle. To compare siRNA-CD98 delivery efficiency by GDLVs with standard methods, we transfected cells with 30 pmol siRNA-CD98 using the Lipofectamine 2000 transfection reagent. To this end, we incubated colon-26 and RAW 264.7 cells for 24 and 48 h with free siRNA-CD98 (30 pmol), siRNA-CD98/Lipofectamine 2000 (30 pmol), GDLVs only or siRNA-CD98/GDLVs (30 pmol). As shown in Figure 8, siRNA-CD98 carried by GDLVs effectively inhibited the expression of CD98 gene by 20.2 ± 5.1% and 21.4 ± 6.2% for 24 and 48 h in colon-26 cells; 66.1 ± 12.9% and 43.0.4 ± 3.0% for 24 and 48 h in RAW cells, which are equivalent to the inhibitory effect of siRNA-CD98 delivered by Lipofectamine 2000 (26.4 ± 3.4% and 5.5 ± 4.5% for 24 h and 48 h in colon-26 cells; 61.4.4.1 ± 12.2% and 31.9 ± 6.6% for 24 h and 48 h in RAW cells). In contrast, GDLVs or siRNA-CD98 alone had no effect on CD98 mRNA expression in colon-26 or RAW 264.7 cells. Collectively, these *in vitro* transfection results show that GDLVs are effective natural vehicles for delivering siRNA-CD98 in different cell lines.

Orally administered siRNA-CD98/GDLVs specifically decrease CD98 expression in the mouse colon

Finally, we sought to investigate whether GDNVs could deliver siRNA-CD98 *in vivo*. First, we used

an IVIS series preclinical imaging system to investigate the *in vivo* biodistribution of orally administered GDLVs labeled with a near-infrared fluorescent dye (DiR). Oral administration offers several advantages for therapies against UC compared with other delivery routes, particularly in terms of access to the target tissue. As shown in Figure 9, GDLVs were effectively retained in the stomach, upper ileum and colon 12 h after oral administration, indicating that GDLVs can be used as a siRNA-CD98 delivery vehicle *in vivo*. By contrast, free DiR only, used as a control, was retained in the stomach, but no DiR fluorescence was observed in the upper ileum or colon. In transfection experiments, siRNA-CD98/GDLV complexes were prepared and orally administered twice (at a 12-h interval). As shown in Figure 10, administration of siRNA-CD98/GDLVs significantly reduced the expression of CD98 in the ileum and colon compared with GDLVs loaded with nontargeting (scrambled) siRNA (negative control). However, no decrease in CD98 expression was observed in the duodenum or jejunum, a finding that is consistent with the results of IVIS imaging, which showed that siRNA-CD98/GDNVs did not exhibit high retention in these parts of the intestinal tract. Collectively, these findings demonstrate the successful oral delivery of GDLVs loaded with functional siRNA-CD98, high retention in the ileum and colon, and siRNA-CD98 mediated suppression of CD98 expression in the ileum and colon. Our results also demonstrate that the effective dose of siRNA-CD98 delivered via GDLVs is approximately 10,000 lower than that for systemically administered naked siRNA-CD98 [15,47].

Conclusion

In this study, we developed a new siRNA-delivery vehicle based on ginger-derived lipids, showing that GDLVs can encapsulate siRNA-CD98 and that orally delivered GDLVs loaded with a very low dose of siRNA-CD98 specifically and efficiently reduce colonic CD98 gene expression. Because GDLVs are more biocompatible and can be produced economically on a large scale, nanovehicles derived from edible plants represent one of the safest and most cost-effective therapeutic delivery platforms. Our results suggest that the resulting siRNA-CD98/GDLVs have the potential to shift the current paradigm of siRNA delivery away from artificially synthesized nanoparticles toward the use of nature-derived nanovehicles from edible plants. As such, our findings expand current perspectives on siRNA-delivery systems by natural nanoparticles and could lay the foundation for a safe siRNA-delivery system for treating UC.

Supplementary data

To view the supplementary data that accompany this paper please visit the journal website at: www.futuremedicine.com/doi/full/10.2217/nnm-2017-0196

Financial & competing interests disclosure

This work was supported by grants from the National Institutes of Health of Diabetes and Digestive and Kidney (RO1 DK071594 to D Merlin; RO1 DK109717 to D Merlin and JF Collins). M Zhang was the recipient of a Research Fellowship Award from the Crohn's & Colitis Foundation of America. D Merlin is a recipient of a Research Scientist Award from thr Department of Veteran Affairs. The authors have no other relevant affiliations or financial involvement with any organization or entity with a financial interest in or financial conflict with the subject matter or materials discussed in the manuscript apart from those disclosed.

No writing assistance was utilized in the production of this manuscript.

Summary points

- To overcome the limitations of synthetic nanoparticles for the delivery of siRNA, we created a novel siRNA-delivery vehicle (ginger-derived lipid vehicles [GDLVs]) from edible ginger lipids.
- GDLVs exhibited excellent biocompatibility both *in vitro* and *in vivo* compared with the control liposome, DC-Chol/DOPE.
- siRNA-CD98/GDLVs complexes reduced CD98 expression with high efficiency in both Raw 264.7 and colon-26 cells.
- Orally administered GDLVs loaded with a very low dose of siRNA-CD98 reduced the expression of CD98, implicated in ulcerative colitis, in the ileum and colon, and thus may be useful for treating ulcerative colitis.
- Our results suggest that GDLVs made from ginger-derived lipids could shift the current paradigm of siRNA delivery away from artificially synthesized nanoparticles toward the use of nature-derived nanovehicles from edible plants.

References

Papers of special note have been highlighted as: • of interest; •• of considerable interest

1 Kaser A, Zeissig S, Blumberg RS. Inflammatory bowel disease. *Annu. Rev. Immunol.* 28, 573–621 (2010).

2 Vavricka SR, Gubler M, Gantenbein C *et al.* Anti-TNF treatment for extraintestinal manifestations of inflammatory

bowel disease in the swiss IBD cohort study. *Inflamm. Bowel Dis.* 23(7), 1174–1181 (2017).

3 Bernstein CN, Blanchard JF, Kliewer E, Wajda A. Cancer risk in patients with inflammatory bowel disease: a population-based study. *Cancer* 91(4), 854–862 (2001).

4 Eaden JA, Abrams KR, Mayberry JF. The risk of colorectal cancer in ulcerative colitis: a meta-analysis. *Gut* 48(4), 526–535 (2001).

5 Neurath MF. Current and emerging therapeutic targets for IBD. *Nat. Rev. Gastroenterol. Hepatol.* 14(5), 269–278 (2017).

6 Sam JJ, Bernstein CN, Razik R, Thanabalan R, Nguyen GC. Physicians' perceptions of risks and practices in venous thromboembolism prophylaxis in inflammatory bowel disease. *Dig. Dis. Sci.* 58(1), 46–52 (2013).

7 Kumar J, Newton A. Colon targeted rifaximin nanosuspension for the treatment of inflammatory bowel disease (IBD). *Antiinflamm. Antiallergy Agents Med. Chem.* 15(2), 101–117 (2016).

8 Razanskaite V, Bettey M, Downey L *et al.* Biosimilar infliximab in inflammatory bowel disease: outcomes of a managed switching programme. *J. Crohns Colitis* 11(6), 690–696 (2017).

9 Dong R, Zheng S, Chen G. The appropriate dose and cost of iron replacement therapy in patients with IBD. *Gut* 66(1), 196–197 (2017).

10 Ghosh S, Louis E, Beaugerie L *et al.* Development of the IBD disk: a visual self-administered tool for assessing disability in inflammatory bowel diseases. *Inflamm. Bowel Dis.* 23(3), 333–340 (2017).

11 Walker JR, Ediger JP, Graff LA *et al.* The Manitoba IBD cohort study: a population-based study of the prevalence of lifetime and 12 month anxiety and mood disorders. *Am. J. Gastroenterol.* 103(8), 1989–1997 (2008).

12 Deepak P, Sifuentes H, Sherid M, Stobaugh D, Sadozai Y, Ehrenpreis ED. T-cell non-Hodgkin's lymphomas reported to the FDA AERS with tumor necrosis factor-alpha (TNF-alpha) inhibitors: results of the REFURBISH study. *Am. J. Gastroenterol.* 108(1), 99–105 (2013).

13 Nielsen OH, Loftus EV Jr, Jess T. Safety of TNF-alpha inhibitors during IBD pregnancy: a systematic review. *BMC Med.* 11, 174 (2013).

14 Fiorino G, Danese S, Pariente B, Allez M. Paradoxical immune-mediated inflammation in inflammatory bowel disease patients receiving anti-TNF-alpha agents. *Autoimmun. Rev.* 13(1), 15–19 (2014).

15 Laroui H, Geem D, Xiao B *et al.* Targeting intestinal inflammation with CD98 siRNA/PEI-loaded nanoparticles. *Mol. Ther.* 22(1), 69–80 (2014).

- **Describes a synthetic nanoparticle to delivery CD98 siRNA to decrease colitis.**

16 Maisel K, Ensign L, Reddy M, Cone R, Hanes J. Effect of surface chemistry on nanoparticle interaction with gastrointestinal mucus and distribution in the gastrointestinal tract following oral and rectal administration in the mouse. *J. Control. Release* 197, 48–57 (2015).

17 Zhang MZ, Xu CL, Wen LQ *et al.* A Hyaluronidase-responsive nanoparticle-based drug delivery system for targeting colon cancer cells. *Cancer Res.* 76(24), 7208–7218 (2016).

18 Xiao B, Zhang Z, Viennois E *et al.* Combination therapy for ulcerative colitis: orally targeted nanoparticles prevent mucosal damage and relieve inflammation. *Theranostics* 6(12), 2250–2266 (2016).

19 Zhang MZ, Yu Y, Yu RN, Wan M, , Zhang RY, Zhao YD. Tracking the down-regulation of folate receptor-alpha in cancer cells through target specific delivery of quantum dots coupled with antisense oligonucleotide and targeted peptide. *Small* 9(24), 4183–4193 (2013).

20 Zhang MZ, Li C, Fang BY *et al.* High transfection efficiency of quantum dot-antisense oligonucleotide nanoparticles in cancer cells through dual-receptor synergistic targeting. *Nanotechnology* 25(25), 255102 (2014).

21 Laroui H, Viennois E, Xiao B *et al.* Fab'-bearing siRNA TNF alpha-loaded nanoparticles targeted to colonic macrophages offer an effective therapy for experimental colitis. *J. Control. Release* 186, 41–53 (2014).

22 Huang Z, Gan JJ, Jia LX *et al.* An orally administrated nucleotide-delivery vehicle targeting colonic macrophages for the treatment of inflammatory bowel disease. *Biomaterials* 48, 26–36 (2015).

23 Zhang M, Viennois E, Prasad M *et al.* Edible ginger-derived nanoparticles: a novel therapeutic approach for the prevention and treatment of inflammatory bowel disease and colitis-associated cancer. *Biomaterials* 101, 321–340 (2016).

24 Zhang MZ, Collins JF, Merlin D. Do ginger-derived nanoparticles represent an attractive treatment strategy for inflammatory bowel diseases? *Nanomedicine* 11(23), 3035–3037 (2016).

25 Hang TTN, Dalmasso G, Torkvist L *et al.* CD98 expression modulates intestinal homeostasis, inflammation, and colitis-associated cancer in mice. *J. Clin. Invest.* 121(5), 1733–1747 (2011).

26 Rietbergen MM, Martens-De Kemp SR, Bloemena E *et al.* Cancer stem cell enrichment marker CD98: A prognostic factor for survival in patients with human papillomavirus-positive oropharyngeal cancer. *Eur. J. Cancer* 50(4), 765–773 (2014).

27 Kucharzik T, Lugering A, Yan YT *et al.* Activation of epithelial CD98 glycoprotein perpetuates colonic inflammation. *Lab. Invest.* 85(7), 932–941 (2005).

28 Sussman DA, Santaolalla R, Strobel S *et al.* Cancer in inflammatory bowel disease: lessons from animal models. *Curr. Opin. Gastroen.* 28(4), 327–333 (2012).

29 Sun CC, Zargham R, Shao Q *et al.* Association of CD98, integrin beta 1, integrin beta 3 and Fak with the progression and liver metastases of colorectal cancer. *Pathol. Res. Pract.* 210(10), 668–674 (2014).

30 Mu JY, Zhuang XY, Wang QL *et al.* Interspecies communication between plant and mouse gut host cells through edible plant derived exosome-like nanoparticles. *Mol. Nutr. Food Res.* 58(7), 1561–1573 (2014).

31 Kansas state University. Kansas Lipidomics Research Center. www.k-state.edu/lipid/lipidomics/profiling.html

32 Zhang MZ, Xiao B, Wang H *et al.* Edible ginger-derived nano-lipids loaded with doxorubicin as a novel drug-delivery approach for colon cancer therapy. *Mol. Ther.* 24(10), 1783–1796 (2016).

•• **Provides detailed information about how to prepare ginger-derived nanolipids for chemotherapy-doxorubicin delivery.**

33 Ju SW, Mu JY, Dokland T *et al.* Grape exosome-like nanoparticles induce intestinal stem cells and protect mice from DSS-induced colitis. *Mol. Ther.* 21(7), 1345–1357 (2013).

34 Zhuang XY, Teng Y, Samykutty A *et al.* Grapefruit-derived nanovectors delivering therapeutic miR17 through an intranasal route inhibit brain tumor progression. *Mol. Ther.* 24(1), 96–105 (2016).

• **Describes an miRNA delivery system based on grapefruit-derived lipids.**

35 Yang JS, Gad H, Lee SY *et al.* A role for phosphatidic acid in COPI vesicle fission yields insights into Golgi maintenance. *Nat. Cell Biol.* 10(10), 1146–1153 (2008).

36 Kooijman EE, Chupin V, de Kruijff B, Burger KNJ. Modulation of membrane curvature by phosphatidic acid and lysophosphatidic acid. *Traffic* 4(3), 162–174 (2003).

37 Popova AV, Hincha DK. Effects of flavonol glycosides on liposome stability during freezing and drying. *BBA Biomembranes* 1858(12), 3050–3060 (2016).

38 Tam YY, Chen S, Cullis PR. Advances in lipid nanoparticles for siRNA delivery. *Pharmaceutics* 5(3), 498–507 (2013).

•• **Gives a detailed description of current situation of lipid nanoparticles for siRNA delivery.**

39 Foged C. siRNA delivery with lipid-based systems: promises and pitfalls. *Curr. Top. Med. Chem.* 12(2), 97–107 (2012).

40 Srinivas R, Samanta S, Chaudhuri A. Cationic amphiphiles: promising carriers of genetic materials in gene therapy. *Chem. Soc. Rev.* 38(12), 3326–3338 (2009).

41 Zhang MZ, Viennois E, Xu CL, Merlin D. Plant derived edible nanoparticles as a new therapeutic approach against diseases. *Tissue Barriers* 4(2), e1134415 (2016).

42 Yang SY, Zheng Y, Chen JY *et al.* Comprehensive study of cationic liposomes composed of DC-Chol and cholesterol with different mole ratios for gene transfection. *Colloid Surf. B* 101, 6–13 (2013).

43 Sato A, Takagi M, Shimamoto A *et al.* Small interfering RNA delivery to the liver by intravenous administration of galactosylated cationic liposomes in mice. *Biomaterials* 28(7), 1434–1442 (2007).

44 Kawakami S, Yamashita F, Nishikawa M *et al.* Asialoglycoprotein receptor-mediated gene transfer using novel galactosylated cationic liposomes. *Biochem. Bioph. Res. Commun.* 252(1), 78–83 (1998).

45 Desigaux L, Sainlos M, Lambert O *et al.* Self-assembled lamellar complexes of siRNA with lipidic aminoglycoside derivatives promote efficient siRNA delivery and interference. *Proc. Natl Acad. Sci. USA* 104(42), 16534–16539 (2007).

46 Li LY, Hou JJ, Liu XJ *et al.* Nucleolin-targeting liposomes guided by aptamer AS1411 for the delivery of siRNA for the treatment of malignant melanomas. *Biomaterials* 35(12), 3840–3850 (2014).

47 Xiao B, Laroui H, Viennois E *et al.* Nanoparticles with surface antibody against CD98 and carrying CD98 small interfering RNA reduce colitis in mice. *Gastroenterology* 146(5), 1289–1300 (2014).

• **Showed that regulated CD98 expression by CD98 siRNA was a reliable way to reduce colitis in mice.**